Materials Transactions, Vol. 43, No. 10 (2002) pp. 2455 to 2462
Special Issue on Superplasticity and Its Applications

Grain Boundary Character and Superplasticity of Fine-Grained Ultra-High Carbon Steel

Tadashi Furuhara, Eiichi Sato [*1], Taichiro Mizoguchi [*2], Shuji Furimoto and Tadashi Maki

Department of Materials Science and Engineering, Kyoto University, Yoshida-honmachi, Sakyo-ku, Kyoto 606-8501, Japan

The characteristics and superplasticity of the $(\alpha + \theta)$ microduplex structures formed by various thermomechanical processings were studied in an ultra-high carbon steel (Fe–1.4Cr–1.0C). After heavy warm rolling of pearlite, an $(\alpha + \theta)$ microduplex structure with equi-axed α grains of 0.4 μm in diameter and spheroidized θ particles of 0.2 μm in diameter is obtained. The α matrix exhibits a recovered structure in which most of α grain boundaries are low-angle boundaries, resulting in rather smaller elongation at 973 K. Heavy cold rolling and annealing of pearlite produces an $(\alpha + \theta)$ microduplex structure which consists of the coarse-grain region ($d_\alpha \sim 0.4$ μm) with high-angle α boundaries and the fine-grain region ($d_\alpha \sim 0.2$ μm) with low-angle α boundaries. Superplasticity in this specimen is slightly better than the warm-rolled specimen. When pearlite was austenitized in the $(\gamma + \theta)$ region, quenched and tempered at the temperature below A_1, an $(\alpha + \theta)$ microduplex structure in which α and θ grain sizes are nearly the same as in the warm-rolled specimen and most of α boundaries are of high-angle one is formed. Such ultra-fine α grains are formed through the recovery of the fine (α' lath martensite + θ) mixture during tempering. This microduplex structure exhibits superior superplasticity. Heavy warm rolling prior to the quenching and tempering improves total elongation further because the distribution of prior γ grain size is more uniform. When cold-rolled pearlite was austenitized and air-cooled, an $(\alpha + \theta)$ microduplex structure with high-angle α boundary is formed. However, since the α grain size was relatively large (ca. 2 μm), its superplastic performance is poor. Finally, more simplification of processing for superplasticity was attempted. Further improvement of superplasticity was achieved by omitting the tempering in the quenching and tempering treatment.

(Received May 15, 2002; Accepted June 12, 2002)

Keywords: *superplasticity, ultra-high carbon steel, microstructure, grain boundary, pearlite, thermomechanical processing, tempering*

1. Introduction

It has been known that superplasticity in ultra-high carbon steels (carbon content is more than 1.0 mass%C) is achieved for the $(\alpha+\theta)$ microduplex structure with fine, spheroidized θ (Fe_3C) particles dispersed in fine-grained α matrix. Sherby *et al.*[1–6] developed such $(\alpha+\theta)$ microduplex structure by rather complicated thermomechanical processing. The process they proposed consists of three parts; (1) heavy hot rolling in the $(\gamma + \theta)$ two phase region after austenitizing; (2) heavy warm rolling at the temperature just below A_1 temperature; (3) quenching and tempering below A_1 after austenitizing in the $(\gamma+\theta)$ region. The present authors studied the microstructure change in the heavy warm rolling, quenching and tempering performed on the specimens with pearlite structure.[7] It was shown that an $(\alpha+\theta)$ microduplex structure containing a large fraction of high-angle α grain boundaries is formed through the recovery of lath martensite structure during the quenching and tempering of (3). It was confirmed that the presence of such high-angle α boundaries are important in terms of grain boundary sliding for superplasticity in an ultra-high carbon steel with $(\alpha + \theta)$ microduplex structures.

The $(\alpha + \theta)$ microduplex structure which exhibits superplasticity can be produced by heavy cold rolling and annealing of pearlite.[8] The present authors[9] recently reported that heavy cold rolling and annealing of pearlite results in the mixture of two kinds of microduplex structures, which are different in the grain sizes of α and θ phases and the character of α grain boundary. However, the superplasticity in the cold-rolled and annealed pearlite has not been studied in detail.

The present study aims to examine the relationship between the α grain boundary character and superplasticity for various $(\alpha + \theta)$ microduplex structures with different α grain boundary character produced by thermomechanical processing in ultra-high carbon steels.

2. Experimental Procedure

The alloys used are commercial bearing steels (SUJ2: Fe–1.0 mass%C–1.4 mass%Cr) of which chemical composition are listed in Table 1. Although the two alloys used are slightly different in composition, the microstructure obtained is nearly the same. A_1 and A_{cm} temperatures determined by dilatometry measurement for the alloy A are 998 K and 1176 K, respectively.

Specimens were austenitized at 1423 K for 3.6 ks and fully transformed to pearlite by isothermal holding at 923 K for 0.6 ks or 0.9 ks, resulting in a fully pearlitic structure. Subsequently four different thermomechanical processes (as shown in Fig. 1) were performed. The process of (a) is the warm rolling of pearlite at 923 K by 90% (WR). (b) is the annealing at 973 K for various periods of time after cold rolling of pearlite by 70–90% (CR + A). In (c), the pearlite structure was austenitized at 1043 K in the $(\gamma + \theta)$ region followed by oil quenching. Subsequently, the tempering at 923 K for

Table 1 Chemical compositions of the alloys used (mass%).

Alloy	C	Si	Mn	Cr	Fe
A	0.98	0.27	0.41	1.44	bal.
B	1.02	0.24	0.37	1.42	bal.

[*1] Graduate Student, Kyoto University, Present address: Honda R&D Co., Ltd. Asaka R&D Center, Asaka 351-8555, Japan.
[*2] Graduate Student, Kyoto University, Present address: Nissin Steel Co., Ltd., Shin-Nanyo 746-0023, Japan.

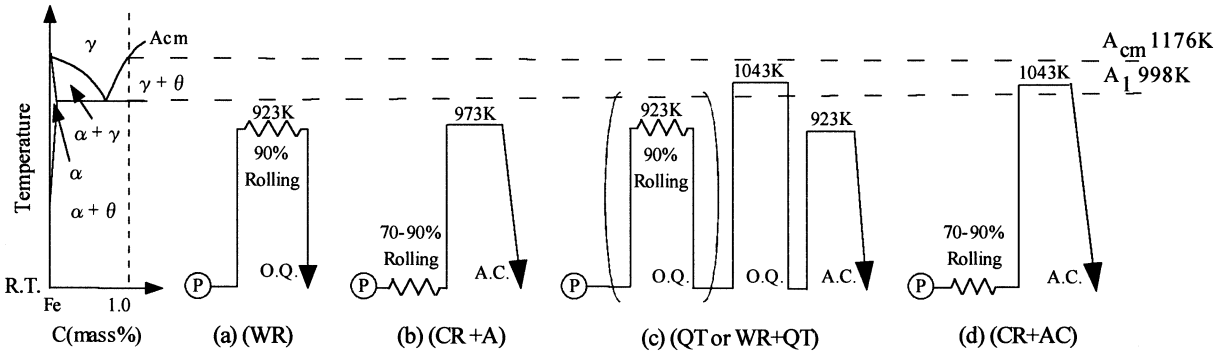

Fig. 1 Thermomechanical processings performed in the present study. (a) 90% warm rolling of pearlite structure at 923 K (WR); (b) annealing at 973 K after 70–90% cold rolling of pearlite structure (CR + A); (c) austenitizing at 1043 K of pearlite structure + quenching + tempering at 923 K without or after 90% warm rolling at 923 K (QT or (WR + QT), respectively); (d) austenitizing at 1043 K after 70% cold rolling of pearlite structure + air cooling (CR + AC).

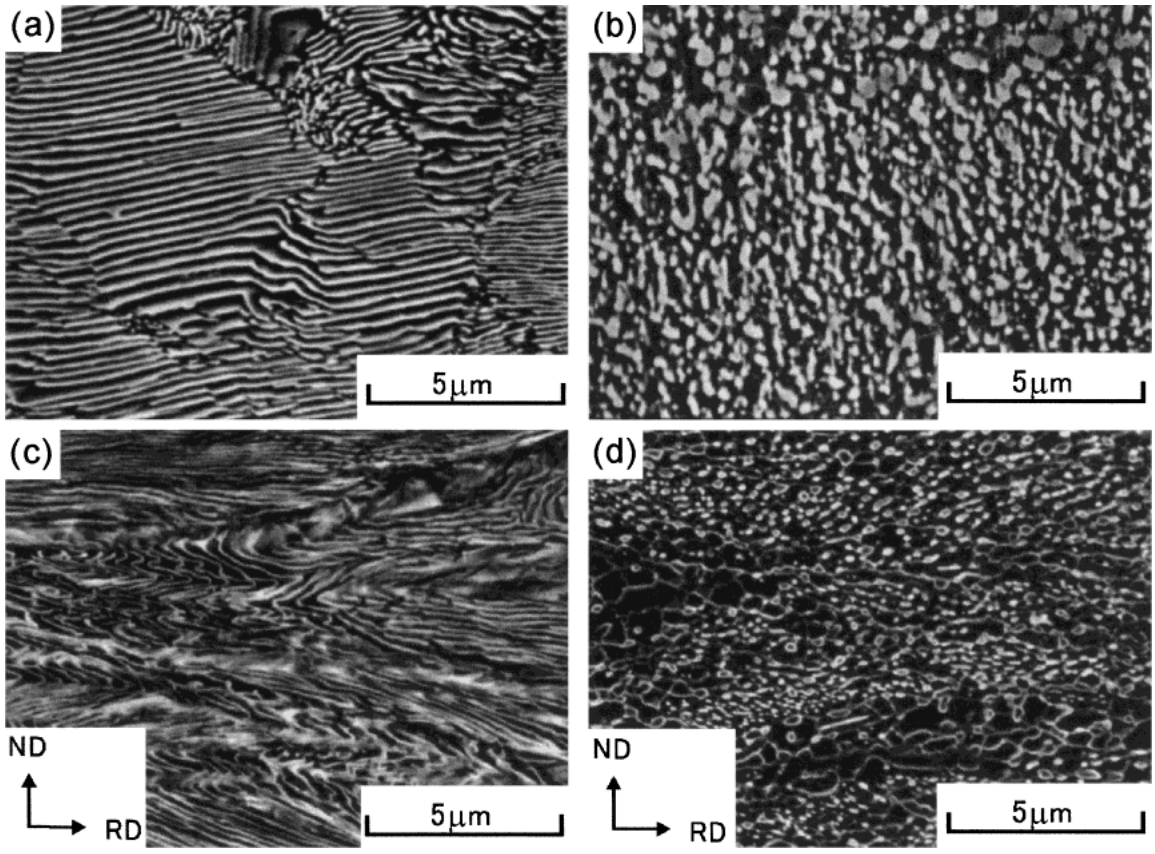

Fig. 2 Microstructure change by the WR and (CR + A) treatments (SEM); (a) as-transformed pearlite, (b) warm-rolled by 90% at 923 K, (c) cold rolled by 70%, (d) annealed at 973 K for 0.6 ks after 70% cold rolling.

various periods of time was performed (QT). In some cases, the warm rolling of pearlite by 90% at 923 K was employed before the quenching and tempering treatment (WR + QT). In (d), the pearlite structure was cold-rolled by 70% and austenitized at 1043 K, followed by air-cooling (CR + AC). Microstructures were observed by scanning electron microscope (SEM: Hitachi S3100H) and transmission electron microscope (TEM: Philips CM200). Orientations of α grains were determined by analyzing convergent beam Kikuchi patterns. Tensile test at 973 K was performed at various initial strain rates between $5.0 \times 10^{-5}\,s^{-1}$ and $1.7 \times 10^{-2}\,s^{-1}$ after heating to 973 K at 1 K/s and holding for 0.6 ks. The gage size of the specimens was $t1.5\,mm \times w2.5\,mm \times l10\,mm$.

3. Results

3.1 The formation process of ($\alpha + \theta$) microduplex structure

The scanning electron micrographs of Fig. 2 show the microstructure change by warm or cold rolling of pearlite structure. Figure 2(a) shows the initial pearlite structure with an interlamellar spacing of about 0.18 μm formed at 923 K. Volume fraction of θ is approximately 15%. By heavy warm rolling at 923 K, initial θ lamellae turn mostly to fine and spheroidized θ particles dispersed in the α matrix (Fig. 2(b)). Figure 2(c) shows that the interlamellar spacing and alignment of lamellae in pearlite turn to be quite non-uniform af-

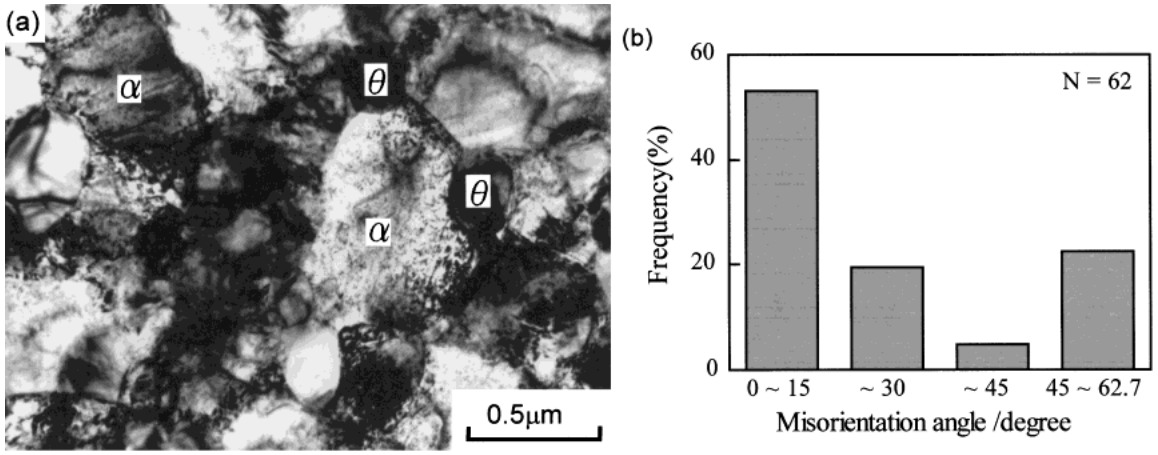

Fig. 3 (a) Transmission electron micrograph of the ($\alpha + \theta$) microduplex structure in the WR specimen and (b) distribution of misorientation angle across α grain boundaries.

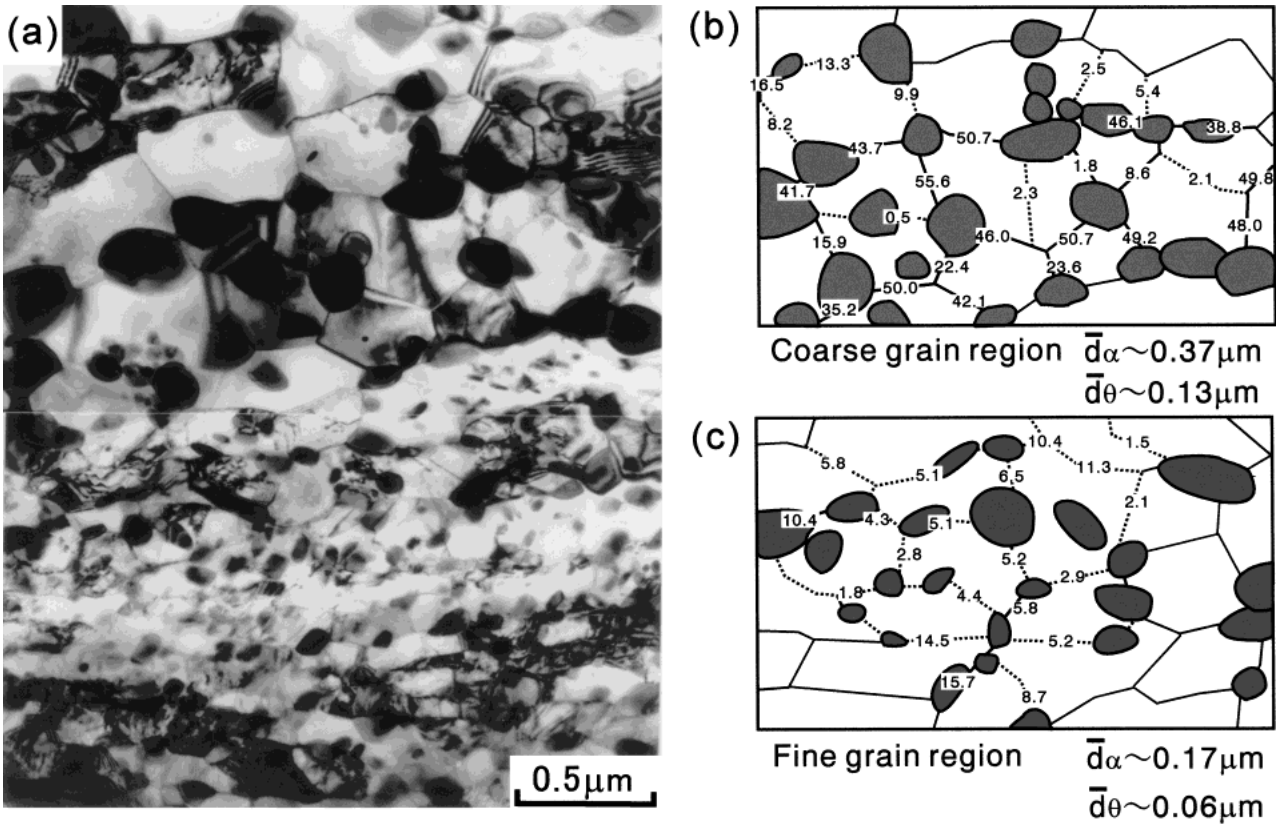

Fig. 4 (a) Transmission electron micrograph of the ($\alpha + \theta$) microduplex structure in the (CR + A) specimen and (b), (c) misorientation angles across α grain boundaries in the coarse-grain and fine-grain regions, respectively.

ter heavy cold rolling as previously reported.[9,10] When heavily cold-rolled pearlite is annealed at 923 K, the microduplex structure consisting of fine α grains and fine θ particles is obtained (Fig. 2(d)). However, the annealed structure is not uniform in the distribution of θ particle size and density because of the heterogeneity in the cold-rolled structure.

Figure 3(a) shows the transmission electron micrograph of the specimen warm-rolled by 90% at 923 K (WR). An ultrafine ($\alpha + \theta$) duplex structure is developed by warm rolling of the pearlite structure. The average α grain size is 0.43 μm and the average θ particle size is 0.18 μm, both in diameter. Figure 3(b) shows the histogram of misorientation angle across the α grain boundary in the warm-rolled specimen. Majority of α grain boundaries are of low-angle one with misorientations less than 15 degrees. Such a low-angle boundary, *i.e.*, the subgrains formed by recovery, is supposed to have a poor ability of grain boundary sliding.

Figure 4 shows the transmission electron micrograph of the ($\alpha+\theta$) duplex structure in the specimen annealed at 973 K for 0.6 ks after 90% cold rolling of the pearlite structure shown in Fig. 2(a) (CR + A) and the corresponding illustrations showing the misorientations across α grain boundaries. In (a), it is clearly seen that the annealed structure consists of the coarse-grain region ($d_\alpha \sim 0.38\,\mu m$, $d_\theta \sim 0.13\,\mu m$) and the fine-

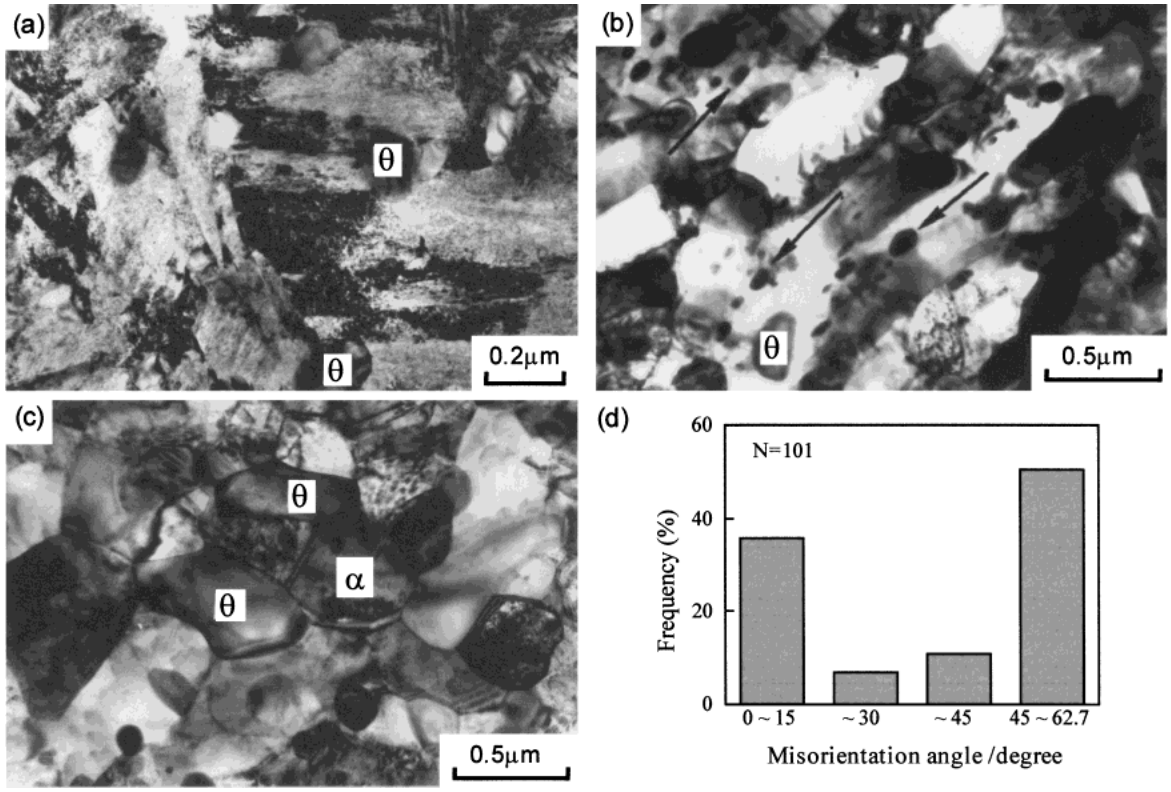

Fig. 5 Microstructure change in the QT treatment; (a) as-quenched, (b) after tempering at 923 K for 0.6 ks and (c) for 1.8 ks, respectively, (d) distribution of misorientation angle across α grain boundaries.

grain region ($d_\alpha \sim 0.17\,\mu m$, $d_\theta \sim 0.06\,\mu m$). Figures 4(b) and (c) show the grain boundary characters for both of those regions. The coarse-grain region in (b) contains many high-angle boundaries with misorientations larger than 15 degrees. On the other hand, most of α grains are subgrains surrounded by low-angle boundaries in the fine-grain region as shown in (c). TEM examination in the early stage of annealing revealed that the area with large misorientation in the deformed α turn to be the coarse-grain region with high-angle α boundaries after recovery during annealing.[9)]

The transmission electron micrographs of Fig. 5 show the microstructure change in the QT treatment. In austenitizing treatment at 1043 K in the $(\gamma + \theta)$ region, the mixture of γ grains and undissolved θ particles is obtained. The average γ grain size is relatively small (11.2 μm) due to the pinning effect by θ particles. By quenching from 1043 K, γ transforms to α' lath martensite. It is known that lath martensite forms "block" (a group of laths with almost the same orientation) and "packet" (a group of laths with almost the same habit plane) structures.[11)] In Fig. 5(a), the growth of lath martensite seems to be stopped by the undissolved θ particles dispersed within the γ grain. As a result, blocks are significantly refined compared with the case without θ particles. After tempering at 923 K (Fig. 5(b)), these undissolved θ particles grow and also new θ particles precipitate in martensite (see the arrows), resulting in a bimodal distribution of θ particle size in the final $(\alpha + \theta)$ structure. Simultaneously, the recovery of lath martensite proceeds to form subboundaries within blocks. Since block or packet boundaries are mostly high-angle boundaries,[12)] the migration of block and packet boundaries occurs in some extent even with the pinning by θ particles. Thus, by further tempering, the shape of α grains changes to equi-axed and, finally, an ultra-fine $(\alpha + \theta)$ microduplex structure with the average grain size of 0.40 μm for α grains and 0.18 μm for θ particles is developed as shown in Fig. 5(c). Those grain sizes are apparently similar to those in the WR specimen. However, the histogram of misorientation angles across the α grain boundaries in Fig. 5(d) indicates that most of α boundaries are of high-angle one with misorientations larger than 15 degrees.

By performing 90% warm rolling before QT treatment, an $(\alpha + \theta)$ microduplex structure with high-angle boundaries similar to the QT specimen was obtained. This process (WR + QT) is comparable to the one proposed by Sherby *et al.*[1)] The average grain sizes were 0.47 μm for α and 0.22 μm for θ. Figures 6(a) and (b) show the optical microstructures of the specimens quenched after austenitizing at 1043 K without warm rolling or after 90% warm rolling of pearlite, respectively. These micrographs reveal the prior γ grains. γ grain size is finer, 6.6 μm in average diameter, and more uniform in the specimen with warm rolling (Fig. 6(b)) than in the specimen without warm rolling (Fig. 6(a)) with the average γ grain size of 11.2 μm. This is probably because the dispersion of θ particle becomes finer and more uniform by the heavy warm rolling. Uniformly distributed fine θ particles should lead to the higher nucleation rate of γ and the larger pinning effect to suppress γ grain growth.

Figures 7(a) and (b) show the scanning and transmission electron micrographs of the specimen of pearlite cold-rolled by 70%, austenitized at 1043 K and air-cooled (CR + AC). During cooling from 1043 K, the duplex structure with spheroidized θ particles and equi-axed α grains is formed by

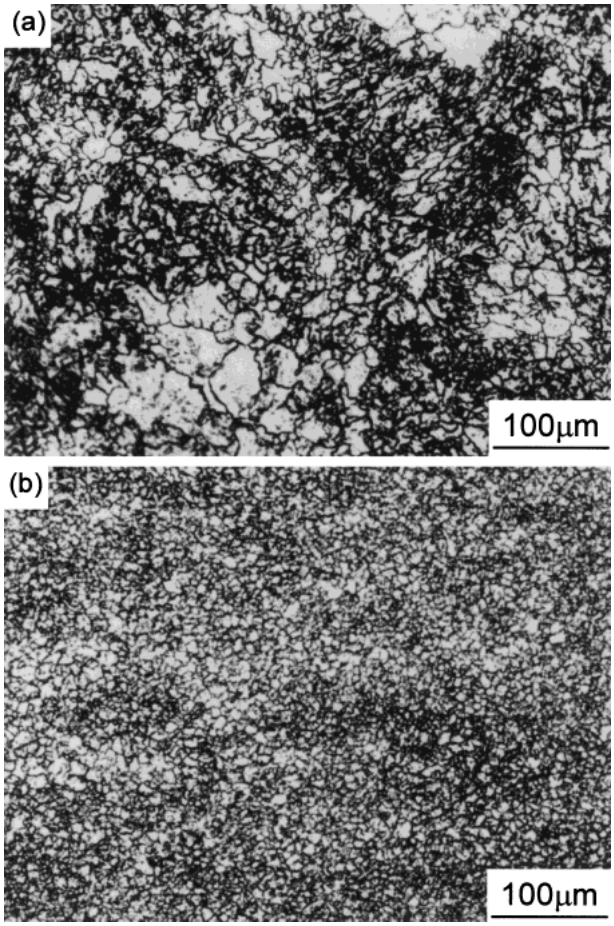

Fig. 6 Optical microstructures of the specimen quenched after austenitizing at 1043 K (a) without warm rolling and (b) after 90% warm rolling, respectively.

the formation of α and the growth of undissolved θ particles. This structure is similar to the "degenerate pearlite" or "divorced pearlite".[13] The average α grain size, 2.0 μm, is larger than the other specimens whereas the average θ particle size, 0.14 μm is about the same as in the other specimens. Figure 7(c) shows that the misorientations across α grain boundaries are large in the area shown in Fig. 7(b). It is considered that α grains neighboring to each other presumably nucleated at different portions of γ grain boundary.

3.2 Superplasticity of the ($\alpha + \theta$) microduplex structure formed by various thermomechanical processings

As was shown in the preceding section, various kinds of ($\alpha + \theta$) microduplex structures were obtained from the initial pearlite structure through thermomechanical processings. The result of tensile test at 973 K for those specimens is summarized in Fig. 8. The QT specimen exhibits more than 500% elongation at the strain rate of $1.7 \times 10^{-4}\,s^{-1}$ although the addition of warm rolling (WR + QT) results in further improvement of superplastic performance. The (WR + QT) and QT specimens which contain large proportions of high-angle α grain boundaries show much better superplastic properties than the WR specimens with low-angle α boundaries (about 300% elongation at the strain rate of $1.7 \times 10^{-4}\,s^{-1}$). In the (CR + A) specimens, two kinds of microduplex structures, *i.e.*, the coarse-grain region with high-angle α boundaries and the fine-grain region with low-angle α boundaries,

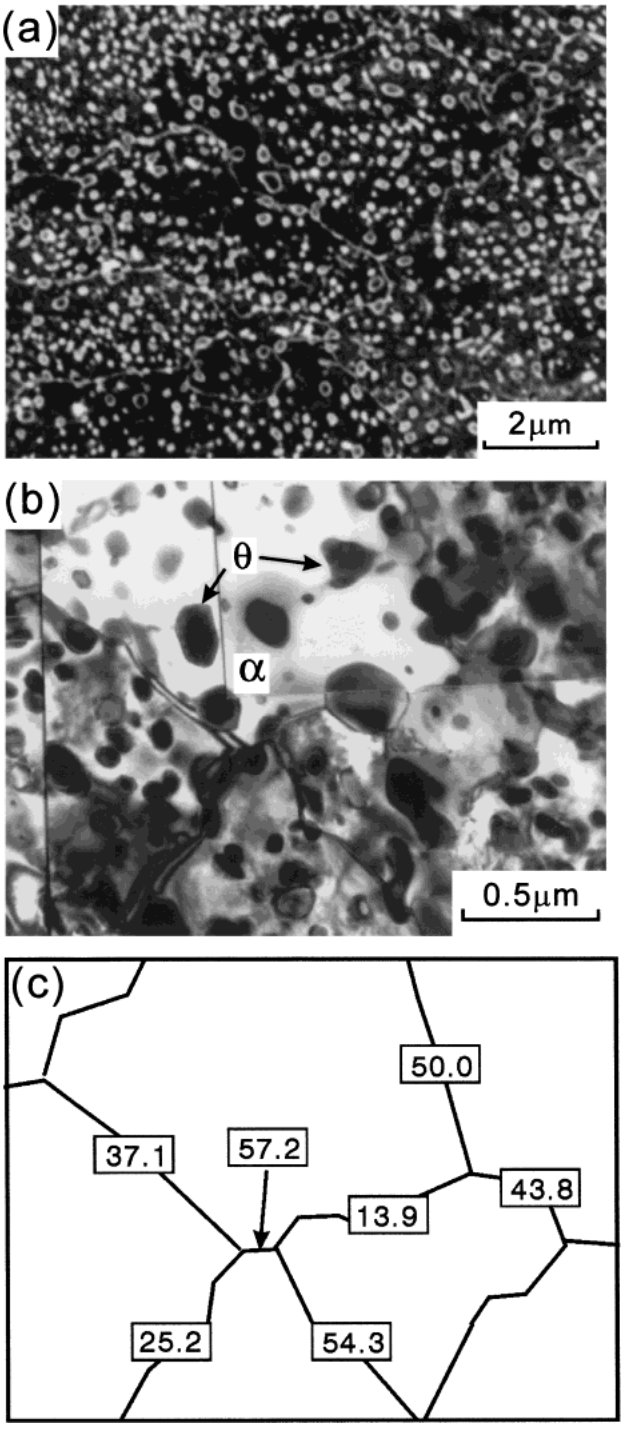

Fig. 7 (a) Scanning and (b) transmission electron micrographs of the ($\alpha + \theta$) microduplex structure in the (CR + AC) specimen and (c) the misorientation angles across α grain boundaries in the area of (b), respectively.

Table 2 Mean strain-rate-sensitivity exponent (m) at 973 K for the specimens on which various thermomechanical processings were performed (between the initial strain rates of $5.0 \times 10^{-5}\,s^{-1}$ and $1.7 \times 10^{-4}\,s^{-1}$ at the true strain of 0.8).

Specimen	WR + QT	QT	WR	CR + A
m-value	0.46	0.54	0.27	0.25

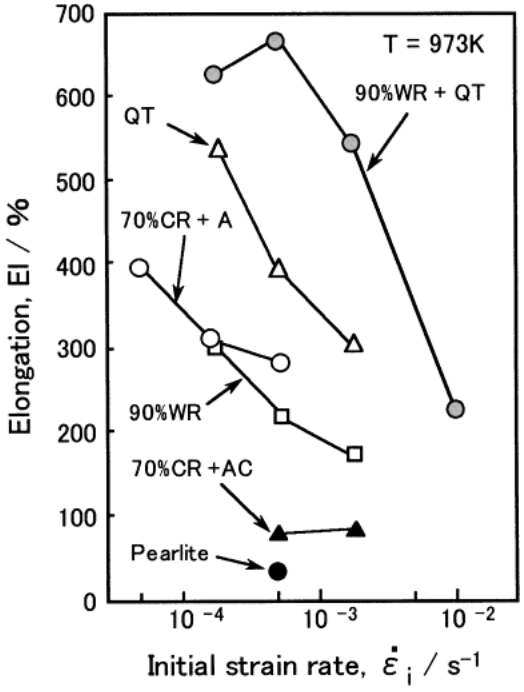

Fig. 8 Elongation to failure of the specimens on which various thermomechanical processings were performed (deformed in tension at 973 K and at various initial strain rates).

are mixed. The resultant superplastic performance is poorer than the (WR + QT) and QT specimens but better than the WR specimen. Table 2 shows the mean strain-rate-sensitivity exponent (m) between the initial strain rates of $5.0 \times 10^{-5}\,s^{-1}$ and $1.7 \times 10^{-4}\,s^{-1}$ at the true strain of 0.8. The m-value is approximately 0.5 for the (WR + QT) and QT specimens, which implies that deformation is controlled by grain boundary sliding.[14] On the other hand, the WR or (CR + A) specimens exhibit the m-value of about 0.25. This result clearly indicates that larger fractions of high-angle α grain boundaries which are capable of grain boundary sliding are of great importance for superplasticity in the ultra-high carbon steels with $(\alpha + \theta)$ microduplex structures. Most of α grain boundaries in the (CR + AC) specimens are of high-angle ones similarly to the (WR + QT) or QT specimens. However, this specimen exhibits poor superplasticity, just slightly better than the initial pearlite, because its α grain size is larger than the other specimens.

4. Discussion

4.1 Origin of high-angle grain boundary in quenched and tempered specimen

The present study clarified the effect of initial $(\alpha + \theta)$ microstructure on the superplastic behavior of an ultra-high carbon steel. The QT treatment produces the $(\alpha + \theta)$ microduplex structure with a large fraction of high-angle α grain boundaries, leading to superior superplasticity. It should be emphasized that, without any complicated deformation at elevated temperature, the $(\alpha + \theta)$ microduplex structure with high-angle α grain boundaries is formed by the QT treatment. Microstructure evolution in this treatment is discussed in the following.

The transmission electron micrographs shown in Fig. 5 indicated that the $(\alpha + \theta)$ microduplex structure with high-angle α grain boundaries is developed essentially through the recovery of lath martensite structure. Figure 9 schematically describes the microstructure transition from the as-quenched condition to the fully tempered condition in the QT specimens. The presence of undissolved θ particles finely dispersed in γ plays an important role in the formation of $(\gamma + \theta)$ duplex structures. By quenching the γ containing finely distributed θ particles, the block and packet sizes are drastically refined. A block corresponds to each fine α grain in the tempering. As a result, the $(\alpha + \theta)$ microduplex structure consisting of α grains smaller than 0.5 μm in diameter and surrounded mostly by high-angle grain boundaries are formed. When the γ contains no θ particles, the blocks and packets of as-quenched lath martensite are much coarser and highly anisotropic in morphology. Under such circumstances, fine equi-axed α grain structures are hardly obtained even after extensively prolonged tempering.[15] The (WR + QT) treatment results in a larger elongation than the QT treatment as shown in Fig. 8. Uniformly dispersed θ particles are obtained after 90% warm rolling and the γ grains are finer and more uniform in size in the austenitizing in $(\gamma + \theta)$ region. Because of this, the $(\alpha + \theta)$ microstructure after tempering should be more uniform in the (WR + QT) specimen compared with the QT specimen, leading to better superplasticity.

In the WR specimens, a majority of α grain boundaries are subboundaries. However, during tensile deformation at 973 K, it was observed that low-angle α grain boundaries in the WR specimens changed to high-angle boundaries through dynamic continuous recrystallization of α as in the case of $(\alpha + \gamma)$ duplex stainless steels.[16,17] Such a transition in grain boundary character might take place in the (CR + A) specimens. Dynamic continuous recrystallization of α occurs by the absorption of dislocations on the subboundaries though recovery and the increase in boundary misorientation. In fact, at slower strain rates for which recovery proceeds more extensively, total elongation at 973 K is larger. However, it appears that such a transition of high-angle boundaries does not occur rapidly enough for superplasticity for higher strain rates.

4.2 Further simplification of the processing for the appearance of superplasticity in ultra-high carbon steel

It was confirmed that high-angle α boundaries in the $(\alpha + \theta)$ microduplex structure is important for the achievement of superplasticity. The origins of high-angle boundaries in the QT specimen are the block and packet boundaries and that in the (CR + A) specimen is the heterogeneity with large misorientations in the deformed structure. During the tempering of QT specimens and annealing of (CR + A) specimens, recovery (not recrystallization) takes place in α matrix besides the precipitation and coarsening of θ. Thus, it was thought that such annealing or tempering treatments could be omitted since isothermal holding at 973 K for 0.6 ks was performed just before tensile deformation to achieve the uniformity of temperature in the specimens.

Figure 10 shows the superplasticity for the more simplified processings. When the tempering in the QT process is omitted, total elongation is increased (see the curve of "Quenching" in the figure). This presumably implies that prolonged

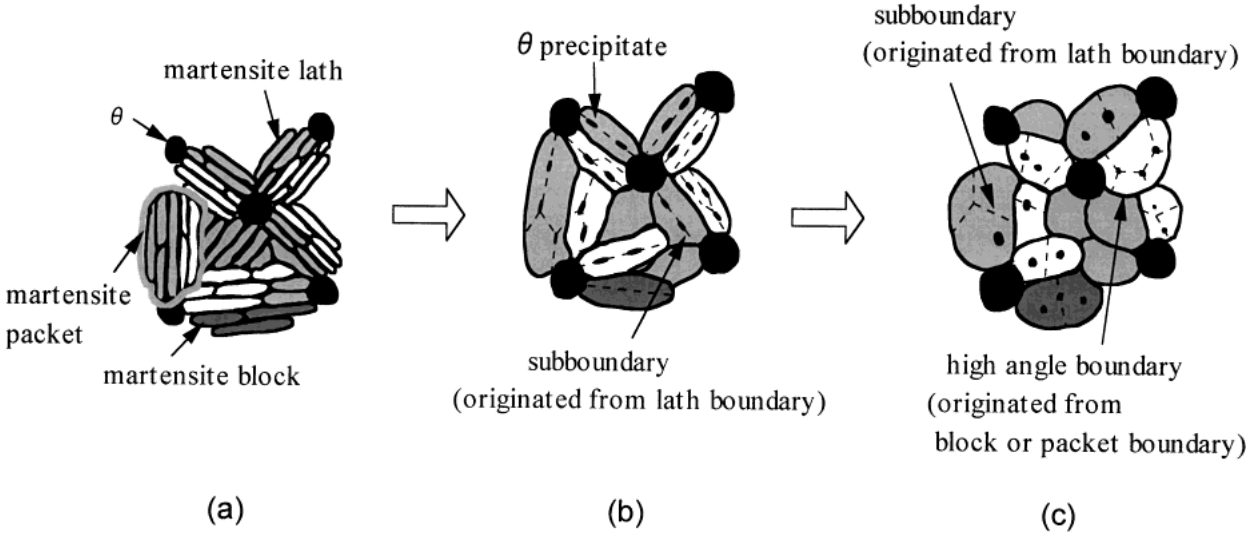

Fig. 9 Formation process of the ($\alpha + \theta$) microduplex structure in the QT treatment.

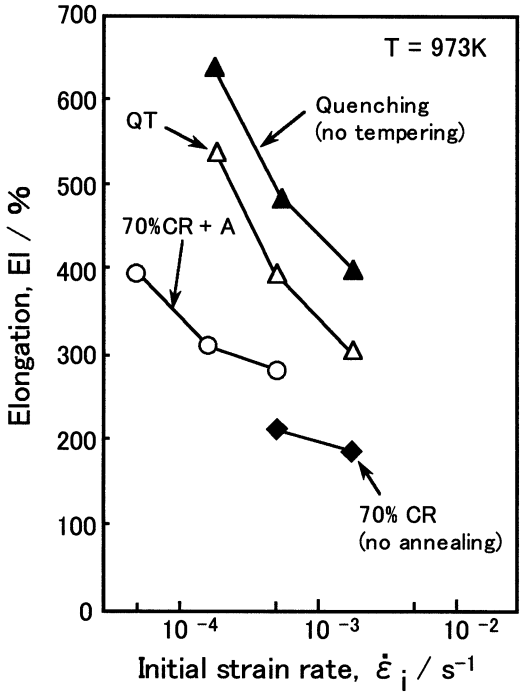

Fig. 10 Effect of simplification in the thermomechanical processing on superplasticity at 973 K.

tempering in QT specimens leads to the coarsening in ($\alpha + \theta$) microduplex structures. On the contrary, elongation becomes smaller when annealing was omitted in the (CR + A) process as seen in the curve of "70%CR". Since the non-uniform distribution of α and θ grain sizes gradually disappeared by increasing annealing time,[18] annealing after heavy cold rolling might lead to the improvement of superplasticity.

5. Summary

The effect of initial ($\alpha + \theta$) microstructures on the superplastic behavior in an Fe–1.0C–1.4Cr ultra-high carbon steel has been studied. The following conclusions were obtained.

(1) By 90% warm rolling of pearlite structure (WR treatment), an fine and equi-axed ($\alpha + \theta$) microstructure with the α grain size of 0.4 μm and the θ particle size of 0.2 μm is obtained. The majority of α matrix exhibits a recovered structure with low-angle grain boundaries, resulting in rather smaller elongation at 973 K.

(2) By austenitizing in the ($\gamma + \theta$) region, quenching and tempering below A_1 temperature (QT treatment), an ($\alpha + \theta$) microduplex structure with the α grain size of 0.4 μm and the θ particle size of 0.2 μm, equivalent to those of WR specimens is obtained. The fraction of high-angle α grain boundary capable of grain boundary sliding significantly increases and large elongation is obtained. α grains surrounded by high-angle boundaries are formed through the following process: (1) the recovery of lath martensite in the fine (α' lath martensite+θ) mixture, (2) the coalescence of α laths in a single block, (3) the morphological transition of α from laths to equi-axed grains.

(3) More simplified processes for superplasticity were attempted. Further improvement of superplasticity was achieved by omitting the tempering in the QT treatment.

REFERENCES

1) J. Wadsworth and O. D. Sherby: J. Mater. Sci. **13** (1978) 2645–2649.
2) O. D. Sherby, B. Walser, C. M. Young and E. M. Cady: Scr. Metall. **9** (1975) 569–573.
3) B. Walser and O. D. Sherby: Metall. Trans. A. **10A** (1979) 1461–1471.
4) O. D. Sherby, T. Oyama, D. W. Kum, B. Walser and J. Wadsworth: J. Metals **37** (1985) 50–56.
5) D. R. Lesure, C. M. Syn, A. Goldberg, J. Wadsworth and O. D. Sherby: J. Metals **45** (1993) Aug., 40–46.
6) T. Oyama, O. D. Sherby, J. Wadsworth and B. Warser: Scr. Metall. **18** (1984) 799–804.
7) E. Sato, S. Furimoto, T. Furuhara, K. Tsuzaki and T. Maki: Mater. Sci. Forum **304–306** (1999) 133–138.
8) K. Seto, T. Kato and H. Abe: Mat. Res. Symp. Proc., **196** (1990) p. 99.
9) T. Mizoguchi, T. Furuhara and T. Maki: Proc. Int. Symp. on Ultra-fine Grained Steels (ISUGS 2001), ISIJ, 2001, p. 198.
10) S. Tagashira, K. Sakai, T. Furuhara and T. Maki: ISIJ Int. **40** (2000) 1149–1155.
11) T. Maki, K. Tsuzaki and I. Tamura: Trans. ISIJ **20** (1980) 207.
12) S. Morito, H. Tanaka, T. Furuhara and T. Maki: Proc. 4th Int. Conf. on Recrystallization and Related Phenomena (RECRYSTALLIZATION 99), (JIM) pp. 295–300.

13) M. Hillert: *The Decomposition of Austenite by Diffusional Processes*, V. F. Zackey and H. I. Aaronson, eds., (Interscience, New York, 1962) pp. 197–247.
14) T. G. Nieh, J. D. Wadsworth and O. D. Sherby: *Superplasticity in metals and ceramics*, (Cambridge University Press, U. K., 1997) p. 32.
15) T. Maki, T. Furuhara and T. Maki: Proc. 19th ASM Heat Treat. Soc. Conf., 2000, (ASM International, Materials Park, OH, U.S.A.) pp. 631–637.
16) K. Tsuzaki, H. Matsuyama, M. Nagao and T. Maki: Mater. Trans., JIM **31** (1990) 983–944.
17) T. Yamazaki, Y. Mizuno, T. Furuhara and T. Maki: Mater. Sci. Forum **304–306** (1999) 127–132.
18) T. Mizoguchi, T. Furuhara and T. Maki: Unpublished Research, 2002, Kyoto University, Japan.